

The Open University's repository of research publications
and other research outputs

Preferably Plinian and Pumaceous: Implications of Microbial Activity in Modern Volcanic Deposits at Askja Volcano, Iceland, and Relevancy for Mars Exploration

Journal Item

How to cite:

Rader, Erika; Simpson, Anna; Amador, Elena; Fraser, Julia M.; Holtzen, Samuel; Hanna, Ashley; Cable, Morgan L.; Cullen, Thomas; Duca, Zach; Gentry, Diana; Murukesan, Gayathri; Rennie, Vincent; Stevens, Adam H.; Sutton, Scot; Tan, George; Cullen, David; Geppert, Wolf and Stockton, Amanda (2020). Preferably Plinian and Pumaceous: Implications of Microbial Activity in Modern Volcanic Deposits at Askja Volcano, Iceland, and Relevancy for Mars Exploration. *ACS Earth and Space Chemistry*, 4(9) pp. 1500–1514.

For guidance on citations see [FAQs](#).

© 2020 American Chemical Society



<https://creativecommons.org/licenses/by-nc-nd/4.0/>

Version: Accepted Manuscript

Link(s) to article on publisher's website:

<http://dx.doi.org/doi:10.1021/acsearthspacechem.0c00015>

Copyright and Moral Rights for the articles on this site are retained by the individual authors and/or other copyright owners. For more information on Open Research Online's data [policy](#) on reuse of materials please consult the policies page.

oro.open.ac.uk

1
2
3
4
5
6
7
8
9
10
11
12
13
14
15
16
17
18
19
20
21
22
23
24
25
26
27
28
29
30
31
32
33
34
35
36
37
38
39
40
41
42
43
44
45
46
47
48
49
50
51
52
53
54
55
56
57
58
59
60

Preferably Plinian and Pumaceous: Implications of microbial activity in modern volcanic deposits at Askja volcano, Iceland, and relevancy for Mars exploration

Erika Rader¹, Anna Simpson², Elena Amador³, Julia M. Fraser², Samuel Holtzer⁴,

Ashley Hanna², Morgan L. Cable³, Thomas Cullen⁵, Zach Duca², Diana Gentry⁶,

Gayathri Murukesan⁷, Vincent Rennie⁸, Adam H. Stevens⁹, Scot Sutton², George Tan²,

David Cullen⁵, Wolf Geppert¹⁰, Amanda Stockton²

¹University of Idaho (erader@uidaho.edu) ²Georgia Institute of Technology ³Jet

Propulsion Laboratory, California Institute of Technology ⁴University of Colorado at

Boulder ⁵Cranfield University ⁶NASA Ames Research Center ⁷University of Turku ⁸Open

University ⁹University of Edinburgh ¹⁰Stockholm University

1
2
3
4 KEYWORDS Astrobiology, Volcanology, Explosive, Geochemistry, Mars, VNIR
5
6
7

8
9 ABSTRACT To search more efficiently for a record of past life on Mars, it is critical to
10
11 know where to look and thus maximize the likelihood of success. Large-scale site
12
13 selection for the Mars 2020 mission has been completed, but small (meter to 10 cm) scale
14
15 relationships of microenvironments will not be known until the rover reaches the surface.
16
17
18

19
20 Over a 2 meter transect at a modern volcanic deposit on the flank of Askja volcano in the
21
22 barren highlands of Iceland, we compared two biological indicators (ATP activity and
23
24 16SrRNA amplicon sequence composition) to physical characteristics including bulk
25
26 chemical composition, spectral signatures of mineralogy, and grain size. Using analytical
27
28 instrumentation analogous to those available on Mars rovers we were able to characterize
29
30 the geological setting of the deposits and link physical parameters to microbial abundance
31
32 and diversity. In general, methanogenesis, methanotrophy/methylotrophy and nitrate reduction
33
34 were the functional traits most associated with microbial community shift along the transect. Core
35
36 microbiome members tended to be associated with nitrate reduction, and relative abundance of
37
38 core microbes were strongly related to free water in the deposit. Community compositional shift
39
40 of the rare microbiome was related to microenvironmental changes such as change in grain size,
41
42
43
44
45
46
47
48
49
50
51
52
53
54
55
56
57
58
59
60

1
2
3
4 geochemistry, and age of deposit. These correlations lead us to suggest a sampling strategy
5
6
7 that accounts for Martian geology, looking for an undisturbed (not-remobilized) explosive
8
9
10 volcanic ash below pumice could maximize diversity and abundance of different
11
12
13 bioindicators. Our study also illustrates the importance of studying the variability across
14
15
16
17 microenvironments in low bio-mass settings on Earth.
18
19
20
21

22 **Introduction:**

23
24
25
26 *Iceland as an Astrobiological Analog* – The highlands of Iceland have low bioabundance
27
28
29 and extensive sandy volcanic deposits, similar to Mars ¹⁻⁵. The chemical and geologic
30
31
32 diversity that develops in this environment is a good representation of the diversity in
33
34
35 surfaces in which ancient lifeforms would have evolved, adapted, and been preserved.
36
37
38
39 The cold, barren, and exposed landscape around the Askja volcano provides a
40
41
42 volcanologically well-constrained event which resulted in physically and chemically
43
44
45 diverse environments in a very compact area, thus excluding effects from microclimates
46
47
48
49 or spatial differences.
50
51
52
53
54
55
56
57
58
59
60

1
2
3
4 *Askja geological background* – The Askja volcano in Iceland lies over the hot-spot-
5
6
7 enhanced mid-ocean ridge that separates the North American Plate to the west and the
8
9
10 European Plate to the east⁴. This lake-filled caldera-forming volcano has historically
11
12
13 erupted everything from mafic effusive lava flows to silicic explosive pumice fall deposits⁶.
14
15
16 Askja had a major catastrophic (Plinian) eruption in 1875 which rained down ash and
17
18
19 pumice which blanketed the northeastern region of Iceland⁶. These deposits still remain
20
21
22 today as unweathered, unaltered, unrounded, and unvegetated layers on top of the wind-
23
24
25
26
27
28 blown sandy desert.

29
30
31 The targeted sampling location contained two primary components, an older aeolian
32
33
34 sandy desert layer (sandur) common in the highlands of Iceland as well as a younger
35
36
37 volcanic fall deposit from the 1875 eruption of Askja volcano ¹. The older volcanoclastic
38
39
40 layer of sediment comprised of wind-blown clasts that covers >20,000 km² is the result
41
42
43
44
45 of harsh weather, high erosion rates, and abundance volcanic source material ¹⁻⁵. This
46
47
48
49 wind-blown mixture of regional volcanic products includes pyroclastics, eroded lava
50
51
52 clasts, and dark colored sand, all of which pre-date the 1875 eruption. The general
53
54
55
56 chemical composition of the sandur is basaltic and made up mostly of glass particles,
57
58
59
60

1
2
3 however, andesitic and rhyolitic are also blown in from the moraines of the Vatnajökull
4
5
6
7 over 30 km away ¹.
8
9

10 On top of the sandur in this location, the 1875 eruption deposited two horizons of a
11
12 deposit called the “C layer” on the 28th-29th of March ^{6, 7}. The C layer is an ash and
13
14 pumice widespread across NE Iceland (see pink outline in Fig. 1) and the thickness
15
16
17 decreases with distance from the vent (Öskjuvatn) as indicated by isopach lines in the
18
19
20
21 same figure ⁸. The grains in the C layer are high in SiO₂, well-sorted, and very angular ⁹.
22
23
24 They are made up of predominantly volcanic glass in the form of sharp pumice fragments ^{10, 11}.
25
26
27 The mineral content of the ash and pumice is ~5% and is made up of plagioclase,
28
29
30 pyroxene, iron oxides and a mention of trace apatite ¹¹. The Askja ash characteristics are
31
32
33 in sharp contrast to the sandur sediment which experienced more collisions with other
34
35
36
37 grains during transport and thus are smaller and more rounded ^{1, 12}.
38
39
40
41
42
43

44 Plinian eruptions, like the one in 1875, are the most violent and explosive of the eruption
45
46
47 classification system developed by ¹³ and often result in wide-spread deposits of ash
48
49
50 and/or pumice ¹⁴. These mega eruptions can produce deposits with basaltic compositions,
51
52
53
54 e.g. ^{15, 16, 17}; however, most are high in silica content, giving a deposit a characteristic
55
56
57
58
59
60

1
2
3 color, mineralogy, and high viscosity which can lead to an extremely large footprint due
4
5
6
7 to the eruption explosivity, e.g. ^{18, 19-21}. Large explosive eruption deposits have been
8
9
10 hypothesized to exist on Mars based on geochemical and morphological indicators, e.g.
11
12
13 ^{22, 23-27}. As relatively low-density pyroclasts can be dispersed extremely far on Earth and
14
15
16 potentially even further in the martian atmosphere, a thin deposit (a bio-
17
18
19 microenvironment) similar to the Askja section could be captured in a stratigraphic section
20
21
22 in a very broad region of Mars, but could be very difficult to identify with the resolution of
23
24
25 satellite imagery currently available ^{28, 29}. With the possibility of encountering a deposit
26
27
28 such as this on Mars, understanding this type of microenvironment could be
29
30
31 advantageous in the search for past life.
32
33
34
35
36
37

38 *Biological background* - On Earth, variations in habitability are best understood by
39
40
41 examining biology directly, for example by examining total biomass or biological activity,
42
43
44 e.g. ^{30, 31}. The use of DNA for information storage and ATP for energy storage are
45
46
47 conserved across all terrestrial organisms ³². Additionally, highly specific and low-limit-of-
48
49
50 detection analytical tools are available for DNA and ATP via fluorescence and
51
52
53 bioluminescence assays, respectively ^{30, 31}. The researchers acknowledge these assays
54
55
56
57
58
59
60

1
2
3 and biomarkers are unlikely to be used for extraterrestrial life-finding missions because
4
5
6
7 they are specifically adapted to the evolutionary history of Earth³³. However, their ubiquity
8
9
10 in terrestrial life and the precision analytical tools available for their analysis means they
11
12
13
14 serve as proxies for biomass and biological activity in low biomass samples ^{30, 31} such as
15
16
17 the Icelandic Plinian pumice deposits. Additionally, community structure and diversity can
18
19
20 be ascertained via metagenomic sequencing of DNA ³⁴, enabling improved understanding
21
22
23
24 of whether an individual sample is ubiquitously habitable across multiple domains of
25
26
27 terrestrial life, or if a sample is dominated by a specific subset of organisms adapted to
28
29
30 survive in a niche environment.
31
32
33

34
35 *Mars background* - Though it now appears that Mars was once habitable e.g. ³⁵ whether
36
37
38 or not it was inhabited is yet to be determined. Several future Mars exploration missions
39
40
41 are tasked with searching for direct evidence of past Martian life. For example, NASA's
42
43
44 Mars 2020 mission will travel to Jezero crater, an ancient deep-basin lake that was active
45
46
47 during Mars' most habitable period, the Noachian (~4.0 Gya). Much of the lake's history
48
49
50 has been inferred by the exposed surface mineralogy determined from visible/near-IR
51
52
53 reflectance spectra and geomorphology determined by high-resolution visible imagery
54
55
56
57
58
59
60

1
2
3 taken from orbital spacecraft, e.g. ^{36, 37}. At Jezero, the Mars 2020 rover will investigate,
4
5
6
7 and then cache, a limited number of surface samples with a suite of instruments that will
8
9
10 allow for the inference of chemistry, mineralogy, and biogenicity. Because only ~40
11
12
13 samples will be collected, the Mars 2020 science team will need to carefully determine
14
15
16
17 from Earth whether a sample is high priority for caching and which samples may have the
18
19
20 highest potential for containing biosignatures. As such, the rover will be equipped with
21
22
23 “stand-off” instruments that will help constrain chemistry and grain size (Supercam, PIXL),
24
25
26
27 textures (PIXL), and organic content (SHERLOC) ³⁸⁻⁴⁰. In order to meet the objectives of
28
29
30 the mission, to identify and cache samples that likely contain biosignatures, it is
31
32
33 imperative that scientists understand (A) which geologic settings and rock types best
34
35
36 create habitable microenvironments that preserve biosignatures, and (B) what “stand-off”
37
38
39 or “remote” measurements can be used to identify these samples when scientists cannot
40
41
42 be on the ground. The Mars 2020 mission is one example of a future mission that will rely
43
44
45 on the understanding of which settings are most suitable for preserving biosignatures and
46
47
48
49 what remotely sensed information will help point to their existence. In the future, there will
50
51
52
53
54
55
56
57
58
59
60

1
2
3 undoubtedly be many more missions either robotic or crewed that will rely on this
4
5
6
7 information.
8
9

10 *Microbiomes on Earth compared to Mars* - One of the main goals of biosignature-related
11
12
13
14 Mars analog research is to investigate microbial mineral preference/microbial weathering
15
16
17 that might leave traces of organics or biotically-produced secondary minerals ⁴¹ that can
18
19
20
21 be used to inform biosignature detection, in a manner that might also be possible on Mars.
22
23
24 Earth analog sites used in astrobiology research share some of the extreme conditions
25
26
27
28 found on extraterrestrial planets and moons, but in almost all cases these sites also
29
30
31 contain niches, conditions or nutrients which we would not expect to find elsewhere in our
32
33
34
35 Solar System. The volcanic highlands of Iceland are unvegetated, basaltic and icy like
36
37
38 Mars, but are relatively less extreme because of the presence of higher atmospheric
39
40
41
42 pressure, liquid water, and deposition of organic carbon from elsewhere.
43
44

45 Distinguishing which sediment microbial community members have biosignature-
46
47
48 relevant or Mars-relevant metabolisms is beyond the scope of amplicon sequencing. In
49
50
51
52 this study we have used low abundance as a rough proxy for astrobiological relevance;
53
54
55
56 highest abundance species are more likely to be responding to availability of moisture or
57
58
59
60

1
2
3 CHNOPS, which even in these “extreme” environments are significantly higher than those
4
5
6
7 found on Mars. Thus, as well as assessing the microbial community as a whole, we have
8
9
10 divided the microbiome into two categories: core (high abundance, >1%) vs rare (low
11
12
13 abundance) microbes; see ^{42, 43, 44}. Often, microbial specialists that weather or degrade a
14
15
16 recalcitrant nutrient source are found within the rare microbiome ⁴⁵. Rare microbes also
17
18
19 might be more likely to have chemolithotrophic metabolisms similar to those possible on
20
21
22 an extraterrestrial body such as Mars; see ⁴⁶.
23
24
25
26
27

28 In addition, as a microbial habitat transitions from temperate to extreme conditions and
29
30
31 microbial community structure shifts to adapt, it is the previously rare species that generally
32
33
34 become the core species of the new microbiome ⁴⁷. No life has so far been found on
35
36
37 Mars, and current consensus is that while microbial life may not now exist there, it may
38
39
40 have been present when the planet’s climate was milder. As Mars’ magnetic field and
41
42
43 tectonic activity dissipated and Mars likely transitioned from warmer and wetter to drier,
44
45
46 colder conditions ⁴⁸, previously rare microbial species likely would have survived the
47
48
49 longest and therefore formed the most recent biosignatures of Martian life. Examining the
50
51
52 rare microbiome and its relationship to mineral properties in a Martian analog such as
53
54
55
56
57
58
59
60

Iceland, which might reflect conditions present during Mars' early transition to a sterile cold world, can give us clues as to which mineral conditions might host traces of similar life on Mars. In this study we compare physical parameters with the microbial community in an unaltered volcanic deposit.

Methods:

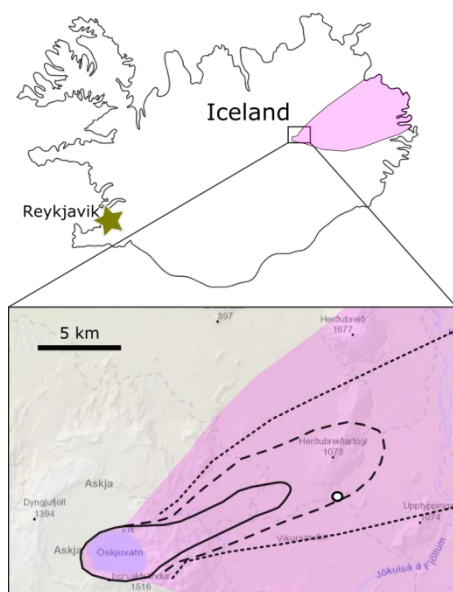


Figure 1. Map of the 0.1 cm thick Unit C deposits of the 1875 Askja eruption in pink. Zoomed in area shows 2.5, 5, and 10 cm thick deposits (dotted, dashed, solid lines) from Carey et al. (2010). Sample location for this study is the small white circle.

Sample collection – A single outcrop exposing a gradation of volcanic layers was selected several kilometers away from the Askja volcano (Fig. 1). The outcrop is about 0.75 meters thick and is exposed along a 100-meter swath that abuts a lava flow margin (Fig. 2A). The low angle of the slope allows for the exposure of about 2 meters of distinctly layered explosive volcanic deposits.

We collected 8 samples across three transects which were about 1.5 meters apart along the outcrop (Fig. 2B).

The bottom two samples were collected from the sandur (Samples EET-1, and 2; Fig. 2C). Three samples (Samples EET-4, 5, and 6; Fig. 2C) were collected from the

1
2
3 extremely fine-grained white ash of the lower C layer^{6, 11}. Two samples were collected
4
5
6
7 from the more coarse-grained, slightly darker fall deposit (upper C) that contains
8
9
10 pumice clasts as well as aeolian basaltic sand (Samples EET-7 and 8; Fig. 2C). Sample
11
12
13
14 EET-3 was a transitional sample that contained material from both layers above and
15
16
17 below.
18
19

20
21 Sampling was completed with extreme care by using sterile gloves, arm guards, and
22
23
24 masks to prevent microbial contamination from the hands, arms, trowels, and
25
26
27
28 respiratory systems of the sample collector. Samplers also positioned themselves
29
30
31 downwind to minimize cross contamination between samples. All surfaces were re-
32
33
34
35 sterilized with ethanol between samples. The top ~3 mm of material was removed to
36
37
38 avoid immediate aeolian contamination. Each sample was excavated 1-5 cm down.
39
40
41
42 The ~ 50 mL of material was sealed in a sterile plastic tube and stored in a cooler during
43
44
45
46 transport to the laboratory where the ATP assay was conducted.
47
48
49
50
51
52
53
54
55
56
57
58
59
60

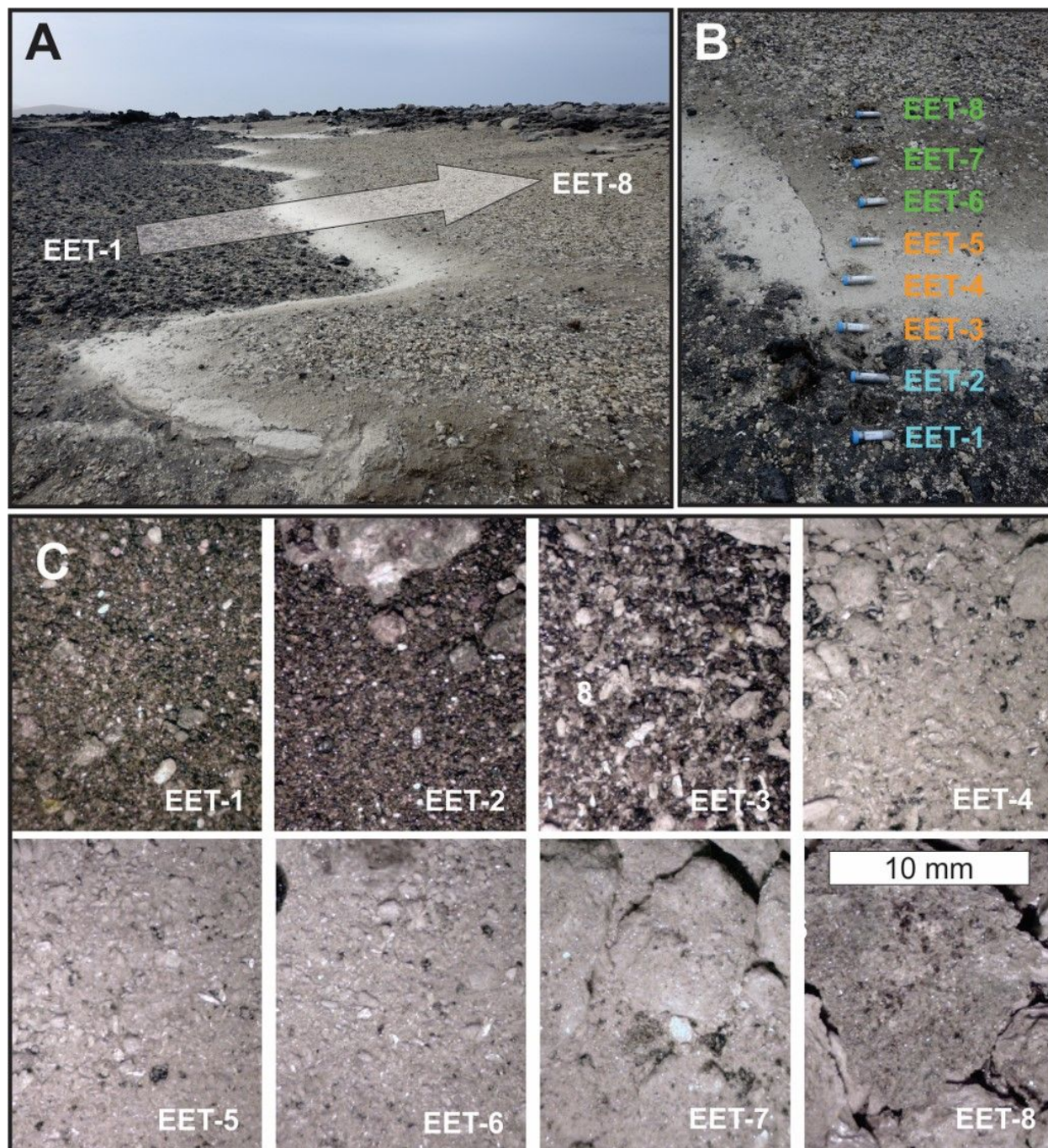


Figure 2. Field location including view of transect of older dark aeolian material below white younger Askja deposit (A). Exact sampling locations (B) as well as close-up images of each sample (C)

“Standoff” mineralogy – Visible and near-infrared (VNIR) (defined here as roughly 350-2500 nm) reflectance measurements are sensitive to minerals that contain transition

1
2
3 metals, such as pyroxenes, and various forms of hydration (OH⁻ and H₂O in
4
5
6
7 phyllosilicates, for example) and can be used to identify the presence of these phases,
8
9
10 even if present at low concentrations. In order to put constraints on the composition of the
11
12
13
14 surface from a distance, we used an Analytical Spectral Devices (ASD) FieldSpec Halo
15
16
17 portable mineral identifier containing an internal broad-spectrum halogen light source. An
18
19
20 external white reference calibration was performed after the instrument warmed up for at
21
22
23
24 least 15 minutes and an internal reference was checked after every 5 collections. Each
25
26
27
28 spectrum collected was an average of 100 scans. An area immediately adjacent to the
29
30
31 collection site was used for ASD analysis; care was taken to ensure that the top layer of
32
33
34 this area was undisturbed, and that the area was similar in physical properties (grain size,
35
36
37
38 color, etc.) to the sample collection site.
39
40

41
42 *Moisture content and grain size analysis* – Moisture content of ~70 mL of sample was
43
44
45 measured by subtracting the dry mass from the collected mass. To obtain the dry mass,
46
47
48 samples were dried in a convection oven at 100 °C for 5 days. After weighing the total
49
50
51
52 sample, the dried sediment was passed through a set of sieves with mesh sizes of 2 mm,
53
54
55
56 0.85 mm, and 0.425 mm. Each grain size group was weighed, and the mass was divided
57
58
59
60

1
2
3
4 by the total giving the mass percent. The sieved fractions of EET-1, 5, and 7 were
5
6
7 photographed and analyzed for roundness with the program ImageJ.
8
9

10 *ATP analysis* - All samples were analyzed within 24 hours of collection. An ATP
11
12 Bioluminescence Assay Kit HSII (Roche Diagnostics Ltd) was used to quantify the ATP
13
14 in the samples. The samples were crushed and homogenized in double layered, sterile
15
16 plastic bags (Whirl-Pak) using a sterilized foil-covered hammer. Tris-EDTA buffer (1 mL
17
18 100mM TRIS, 4mM EDTA) was added to ~0.5 mL of weighted sample each in triplicate,
19
20
21 then boiled for 5 minutes to lyse cells. The suspension was cooled to room temperature
22
23
24 and assayed with the ATP kit. A HY-LiTE 2 luminometer (Merck, VWR International Ltd)
25
26
27 was used to quantify the luminescence. A standard curve was established using known
28
29
30 standards of pure ATP in buffer prepared and analyzed on the same day with the same
31
32
33 reagents.
34
35
36
37
38
39
40
41
42
43
44

45 *Extraction and analysis of DNA sequencing data* – DNA was extracted from transect
46
47
48 sediment samples in triplicate using a low-biomass protocol developed for MOBIO's
49
50
51 PowerSoil kit ⁴⁹. DNA concentrations were measured using a Qubit 2.0 Fluorimeter
52
53
54 (Invitrogen) and Qubit quantitation kits. Reads were scaled to the lowest number of reads
55
56
57
58
59
60

1
2
3 of any sample and transformed sequence numbers to percent abundance. Percent
4
5
6
7 abundance of phyla and proteobacterial classes were calculated for each transect
8
9
10 position and used one-way ANOVAs with Benjamin-Hochberg correction to test for
11
12
13 differences in abundance among mineralogical and geochemical gradients.
14
15

16
17 *Statistical analysis of microbial community correlation with geochemistry* - To examine
18
19
20 changes in the microbial community with mineralogy, microbial community members (i.e.
21
22
23 amplicon sequence variants) were divided into four categories by percentage of total
24
25
26
27 sequences representing each member:
28
29

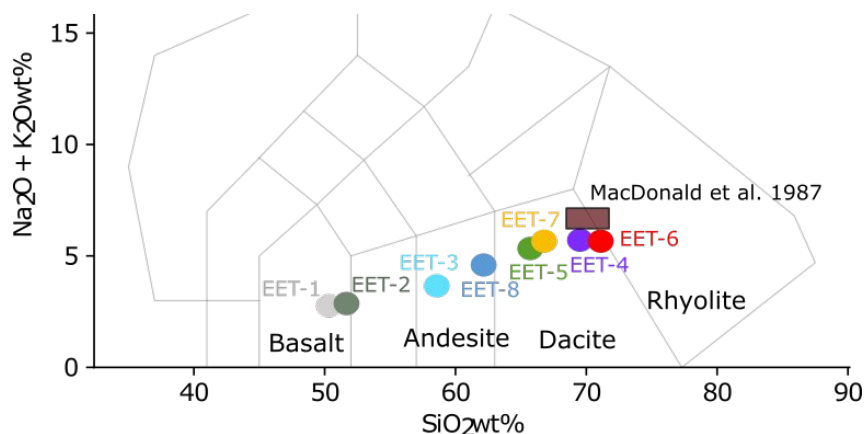
- 30
31 1. Core microbiome (>1%, and present in >20% of samples)
32
33
34 2. High abundance microbiome (>0.1%)
35
36
37
38 3. Medium abundance microbiome (High abundance microbiome excluding
39
40
41 members of the core microbiome)
42
43
44 4. Rare microbiome (<0.1%)⁴²⁻⁴⁴
45
46
47
48

49 A one-way PERMANOVA with Bray-Curtis and Unifrac distance measures was used to
50
51
52 test which environmental variables significantly predicted variation in the microbial
53
54
55
56 community members both overall and in each abundance category. The relative
57
58
59

percentages of sequences belonging to rare ASVs vs core ASVs along the transect was also tested.

To further explore how the rare microbiome was shifting with mineralogy, a differential count analysis using the DESeq2 package⁵⁰ was performed to identify ASVs in the rare microbiome responsible for that shift, using the SiO₂ XRF fraction as a proxy for all mineralogy changes. The ASVs were summed at the genus, family, order and class level and re-performed DESeq2 to evaluate any large-scale taxonomic shifts.

Bulk geochemical analysis – The major elemental geochemistry was analyzed for the whole rock samples by X-Ray fluorescence at the Washington State University Geoanalytical Lab. The remainder of the material after DNA analysis in the triplicate sample tubes were combined, powdered, fused with lithium tetraborate in graphite crucibles in a muffle furnace, repowdered, and re-fused into 3 cm discs. The smaller discs



were used due to limited mass of material remaining after biological analyses. Error for this method is

1
2
3 better than 0.001 wt. % at the 2σ envelope for all analyzed elements as reported by the
4
5
6
7 Geoanalytical Lab.
8
9

10 Results:

11
12
13
14 *Sample descriptions and bulk geochemical analysis* – Samples contained differing
15
16
17 proportions of volcanic ash, scoria, pumice, and aeolian sediment. The stratigraphically
18
19
20 lowest and oldest samples (EET-1 through 3) contained the most scoria and aeolian
21
22
23

24
25 **Figure 3.** Bulk geochemical compositions of each sample plotted on the total
26 alkali-silica diagram.

27
28
29
30
31
32
33
34
35
36
37
38
39
40
41
42
43
44
45
46
47
48
49
50
51
52
53
54
55
56
57
58
59
60

5. Up-section, samples EET-6 through 8 contained increasing amounts of pumice. The
60

normalized oxides wt. % of the samples collected are presented along with the totals in
Table 1. Major elemental totals were between 97.81 and 99.05 wt. % for all samples

except EET-5 which had a total of 90.44 wt. %. The lowest total was due to the loss of
volatile species (Cl and SO_3) during the process of fusing the samples into discs and

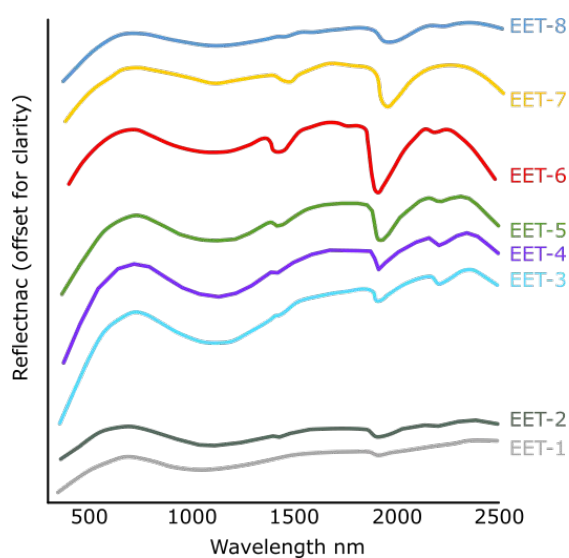
hence, the values for EET-5 should be considered sub-quantitative and not directly
comparable to the rest of the analyses. The stratigraphically lowest samples (EET-1 and

2) are the most mafic (highest FeO wt. %) and have basaltic compositions whereas EET-6

has the most felsic compositions (highest SiO₂ wt. %) and falls close to the rhyolite field on a total alkali-silica diagram (Fig. 3). Samples EET-3 and 8 are andesitic in average composition as they have mixtures of both mafic and felsic material whereas EET-4, 5, and 7 are dacitic.

VNIR characteristics - Reflectance spectra in the visible to near-infrared wavelengths

(300-2500 nm) show absorptions centered around 1400 nm and 1900 nm consistent with



H₂O and OH, and an absorption around 2100 nm

consistent with Si-OH bonds, as well as a broad

absorption in the 1100 nm region also consistent

with silica (Fig. 4). The narrow 1400 nm and 1900

nm absorptions were deepest in EET-6 and 7 while

Figure 4. Spectral characteristics of the visible near-infrared (VNIR) of the samples, offset for clarity.

EET-3 and 4 showed the strongest absorption at

the ~2100 nm. A shift to longer wavelengths in the

1100 range from 1110 nm to 1170 nm can be seen up the transect (Fig. 4). These

absorptions are captured by a set of summary parameters (Table 2) used to detect and

quantify known absorptions related to specific mineral phases, e.g.⁵¹. The raw data is

presented in Table S1. The summary parameters which correlate positively in the lower sandur samples (EET-1 and 2) were those associated with mafic clay minerals (e.g. BD2300, BD2165, and BD 2355) and primary minerals like plagioclase (BD1300) and pyroxene (L and HCPINDEX). The upper Askja samples correlate with hydration indicators like SINDEXT2 and BD1900_2 (Table 2).

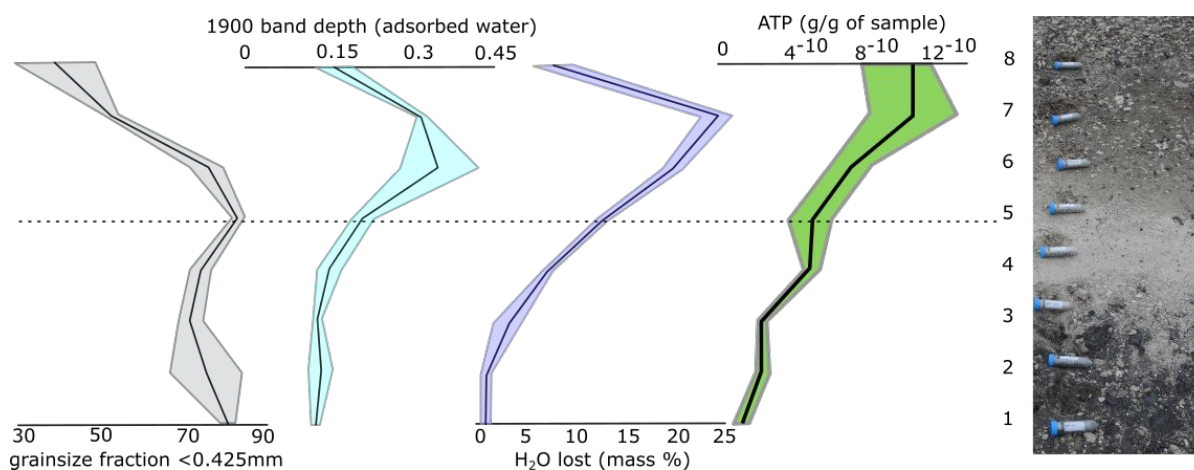


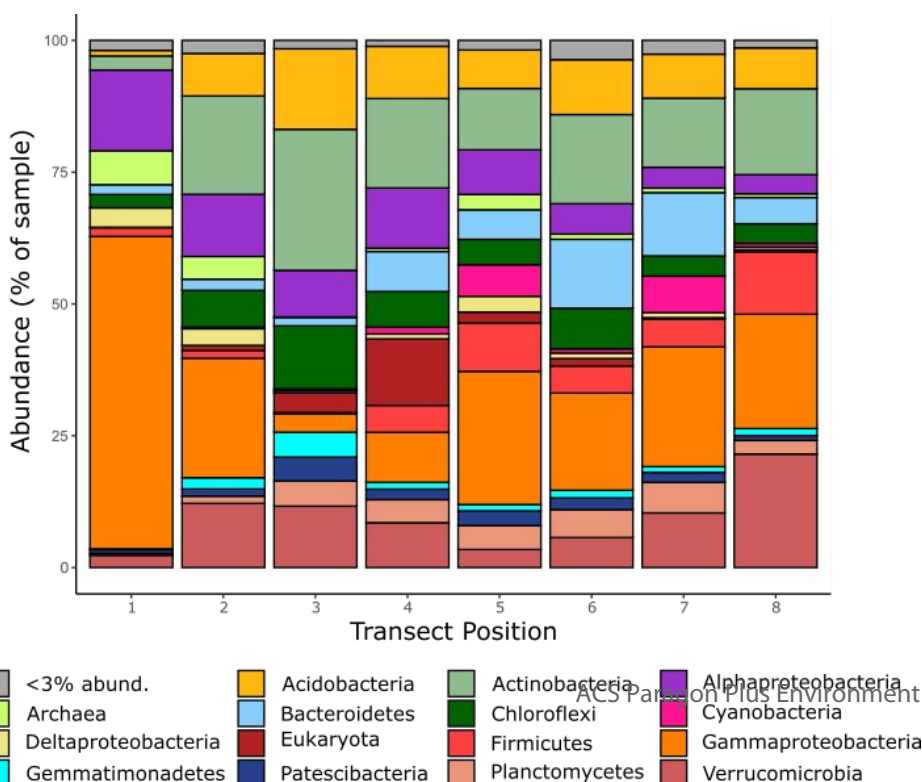
Figure 5. Grain size, water content (adsorbed and free water) and overall ATP for each sample shown next to a photo of the transect. The colored envelope represents the error with the solid line representing the average for each sample. The dashed line references sample 5 in each graph.

Grain size and moisture analysis – Samples included only the particles that could fit inside the sampling tube, which was ~3 cm wide, however, there were very few clasts that were larger than that at all the sites except EET-7 and 8. These samples had larger pieces of pumice that ranged up to ~10 cm in diameter and made up approximately 5% of the surface area of the sampling location based on imagery but were excluded from all

biological and geological analyses (Fig. 2, Table 1). The proportion of the two finest grain sizes (<0.85 mm) ranged from 81-89% in lowest samples (EET-1 through 6) with EET-5 having the higher proportion of fines in the finest grain size (<0.425 mm; Fig. 5). This was in stark contrast to EET-7 and 8, which only had 56% and 46% fines, respectively. These two samples also had a much higher proportion of grains over 2mm in size with 33% and 42%, respectively, compared to the rest of the samples, which had less than 14% >2 mm grains. The samples with the highest moisture content were located directly above the finest grain-sized layers (Fig. 5). Photos of the sieved grains of EET-1, 5, and 7 were analyzed for roundedness and an ANOVA test revealed the grains in EET-1 to be significantly more rounded (average of 0.75) than in the fresh Plinian eruptive material

(average of 0.65; F-statistic: 8.537 on 1 and 10 DF, p-value: 0.01525).

ATP analysis - The ATP measured for the transect samples ranged from 1E-10 to



1
2
3 1E-9 grams of ATP per gram of sediment, with the lowest measures observed in samples
4
5
6
7 EET-1. In successive samples, ATP content increased with samples EET-4 and 5 having
8
9
10 an average measure of 5E-10 g/g, and again in samples EET-7 and 8 with an average
11
12
13
14 measure near 1E-9 g/g (Fig. 5).
15

16
17 *Sequencing results* - The microbial community was dominated by the class
18
19
20
21 Gammaproteobacteria (25% of all sequences) and the phylum Actinobacteria (15% of all
22
23
24 sequences), with secondary dominance of the Acidobacteria, Alphaproteobacteria, and
25
26
27 Verrucomicrobia (8-10% abundance each) (Fig. 6). Almost all members of Archaea were
28
29
30
31 methanogens of the phylum Euryarchaeota.
32

33
34
35 After scaling reads to the minimum number of sequences per sample, samples
36
37
38 contained 2855 unique ASVs, <1% of which made up the core microbiome (>1% of all
39
40
41

42 *Figure 6. Relative abundances of phyla/classes, after reads were scaled to the lowest* sequences within each sample
43 *number of sequences per sample*

44
45 and present in 20% or more of samples) and 70% of which made up the rare microbiome
46
47
48 (<0.1% of all sequences within each sample). Abundant members of the microbiome
49
50
51
52 included ASVs affiliated with denitrification, methylotrophy, and acetoclastic
53
54
55
56 methanogenesis (Table S2).
57
58
59
60

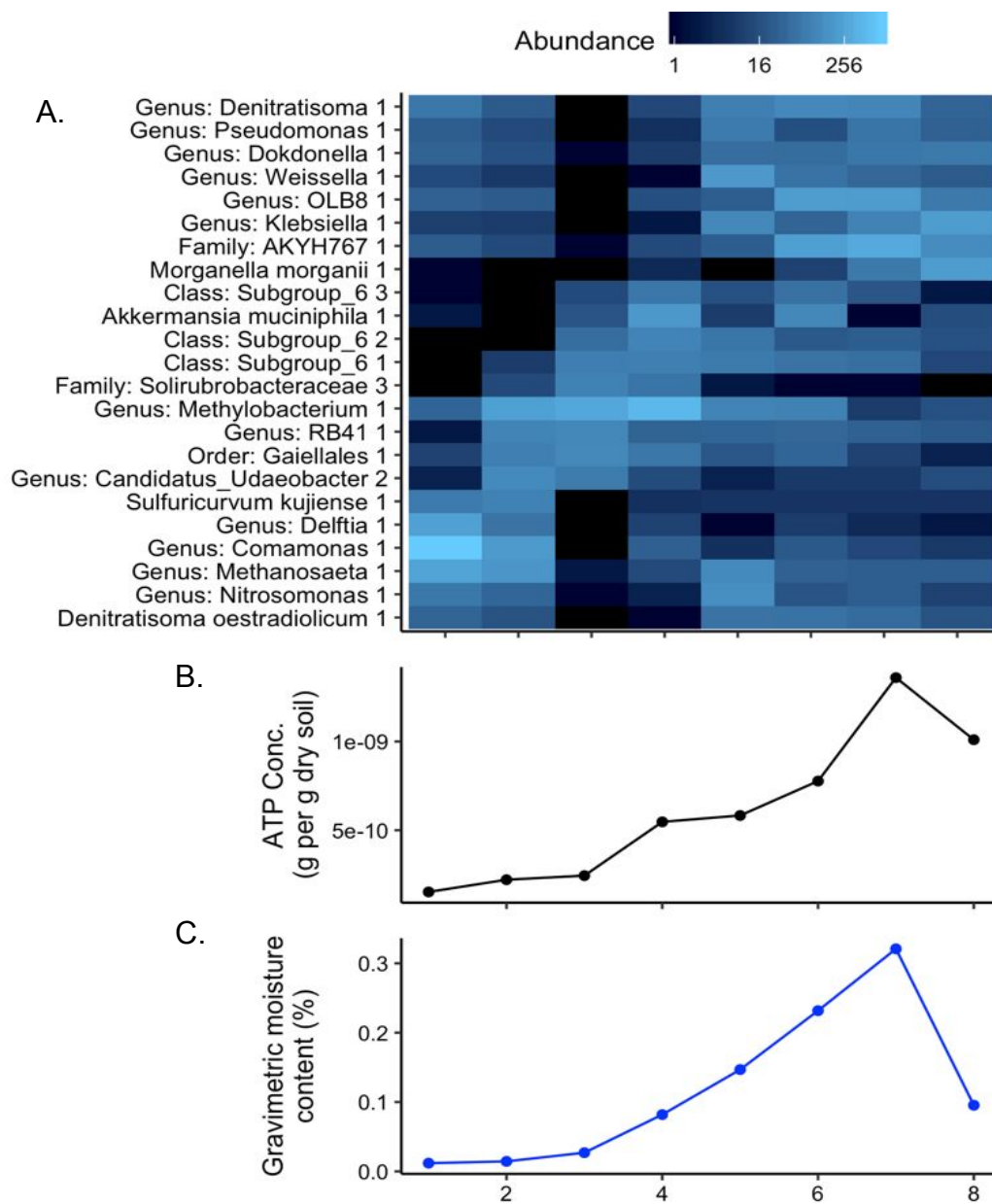


Figure 7. A) Heat map of abundances of amplicon sequence variants (ASVs) which were present in more than 20% of samples and were represented by more than 50 sequences per sample, when sequences are scaled to the lowest number of sequences per sample. Samples are in the order in which they were collected across a mineralogical transect. Below, B) ATP concentration and C) gravimetric moisture content values across the transect.

There were four significant changes in summed phylum abundance of the total microbiome along the transect, divided into categories of older (EET 1 and 2), mixed (EET

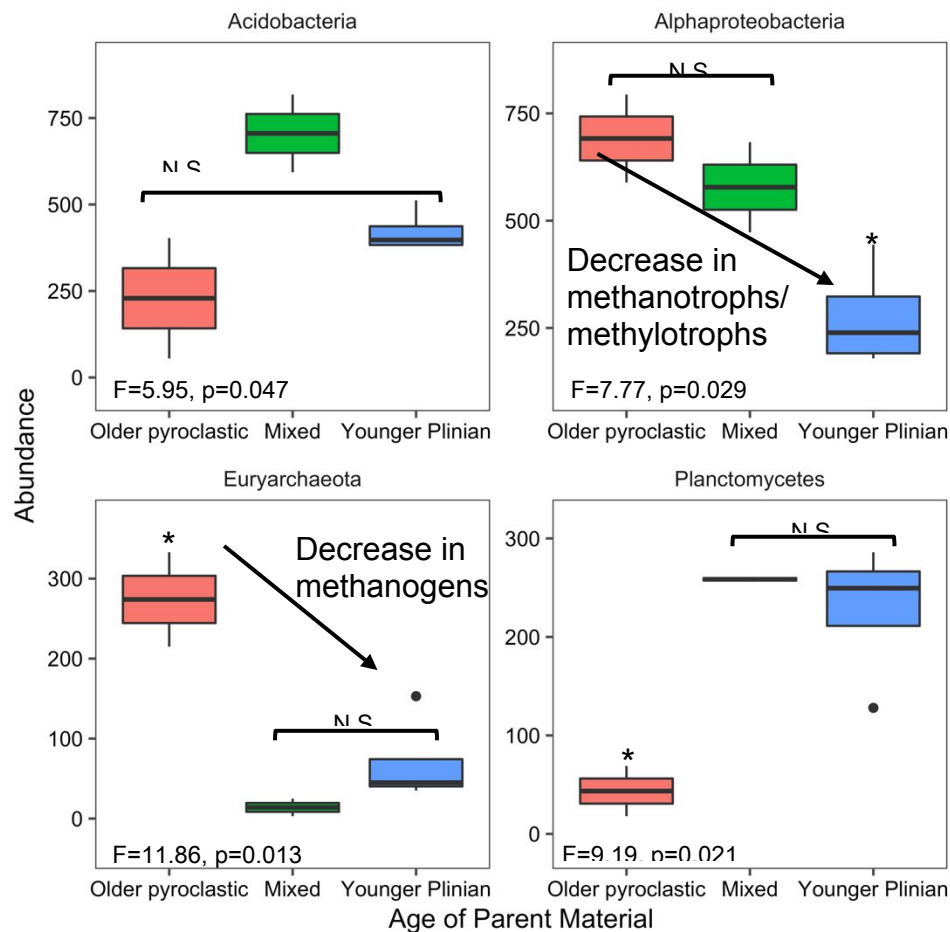
1
2
3 3 and 4, at the transition zone) and younger Plinian parent material (EET 5-8), after
4
5
6
7 Benjamin-Hochberg p-value correction (Fig. 7). Acidobacteria abundance was highest in
8
9
10 the transition zone. Abundance of the Alphaproteobacteria and Euryarchaeota was much
11
12
13 lower in the mixed and younger samples compared to the older samples, while
14
15
16
17 Planctomycetes were more abundant in the mixed and younger parent material zone.
18
19

20
21 Core microbiome relative abundance was significantly predicted by ATP concentration
22
23
24 (i.e. biological activity; $df=7$, $pseudoF=3.282$, $p= 0.006$) and moisture content ($df=7$,
25
26
27 $pseudoF= 2.563$, $p= 0.038$) of the sediment (Table 3, Fig. 7). Shift in the high-abundance
28
29
30
31 microbiome was also predicted by ATP concentration. In contrast, relative abundance of
32
33
34 the rare microbiome was not predicted by biological activity or moisture, but was
35
36
37 significantly predicted by bulk geochemistry of the sediment and by the fractional
38
39
40
41 abundance of sediment grains between 425 μm and 850 μm (Table 3).
42
43
44

45
46 Phylogenetic shift (i.e. use of Unifrac distances in PERMANOVA) was only significantly
47
48
49 predicted in medium-to-high abundance microbes (excluding the core microbiome), by
50
51
52 the fractional abundance of sediment grains between 425 μm and 850 μm ($df=7$,
53
54
55
56
57
58
59
60

pseudoF= 2.295, $p= 0.018$). Abundance of certain phyla also varied greatly depending on the age of the material (Fig. 8).

Differential count (DESeq2) analysis of the rare microbiome did not yield any ASVs or genera that shifted significantly from low to high silica content after Benjamin-Hochberg correction of p values – this was unsurprising given that each individual ASV was of low abundance. When



1
2
3 **Figure 8.** *Phyla with significant differences in abundance with age of parent material, as tested by one-way ANOVA*
4 *with FDR p-value correction. The decrease in Alphaproteobacteria is mainly due to the decrease in one sequence for*
5 *a methanotroph / methanol consumer, and the decrease in Euryarchaeota is due to the decrease in two sequences,*
6 *one an acetoclastic methanogen (genus Methanosaeta) and one a methanogen that can form methane from either*
7 *formate or H₂ and CO₂ (genus Methanobacterium).*
8
9

10 summed across different taxonomic levels, the families Hydrogenophilaceae and
11
12
13
14 Caulobacteraceae, both in the phylum Proteobacteria, were significantly more abundant
15
16
17
18 in low silica samples and the order Rhizobiales was significantly more abundant in high
19
20
21
22 silica samples.
23

24 **Discussion:**

25
26
27
28 *1. Geological observations.* The Plinian eruption at Askja in 1875 produced a well-
29
30
31 sorted fine-grained fall deposit followed by a more pumice-rich fall deposit which we
32
33
34 examined geochemically and mineralogically using measurements similar to those that
35
36
37 are currently, or planned to be available on Mars with robotic missions. Additionally, we
38
39
40 examined the biological patterns associated with these deposits in an effort to inform
41
42
43
44
45 sampling protocols to maximize the recovery of bioindicators in volcanic terrains.
46
47
48

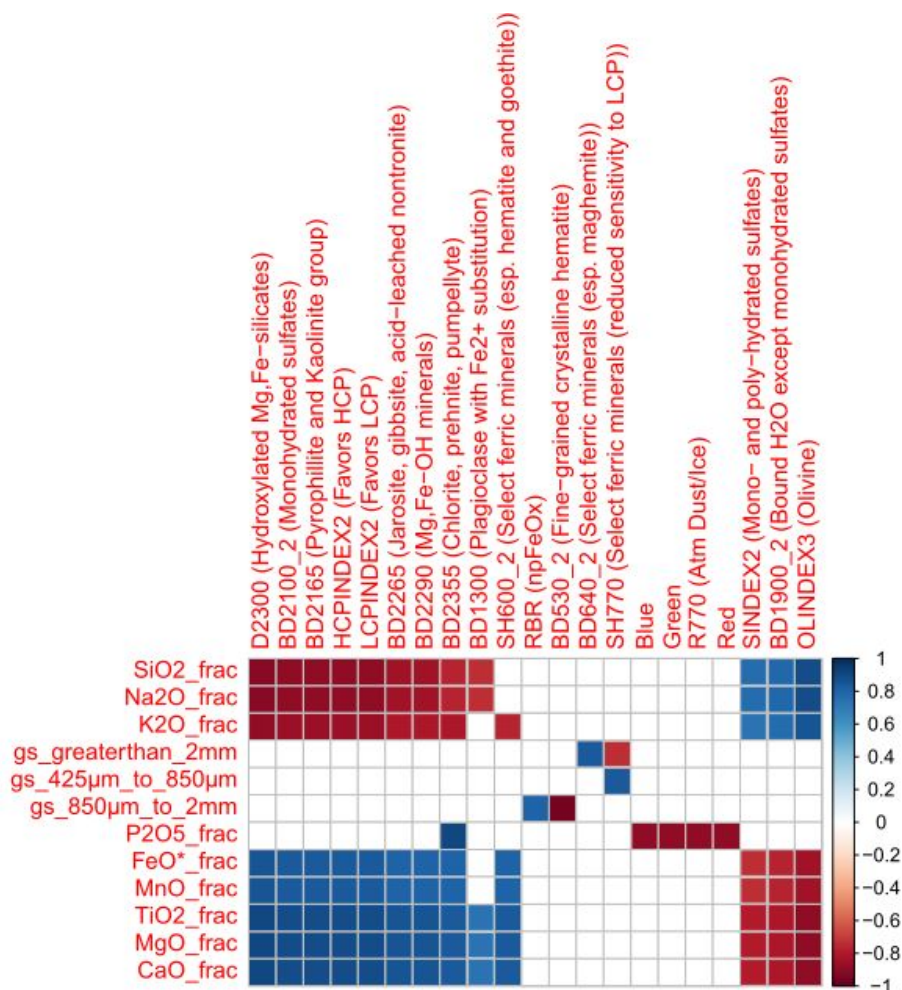
49 *VNIR and XRF characteristics of explosive eruptions* - An explosive eruption on Earth
50
51
52 often results in deposits of fine-grained glassy particles with some components of pumice
53
54
55
56
57
58
59
60

1
2
3 and crystals. While this determination can be made from a small sample of material alone,
4
5
6
7 it can be helpful to have microanalytical techniques as well as field relationships with
8
9
10 surrounding units ⁵². As this might be limited by orbital resolution context imagery and
11
12
13
14 with the narrow mobility of rover or crewed missions to Mars, we focused our
15
16
17 characterization of these deposits on up-close imagery, VNIR, and XRF analysis.
18
19

20
21 Color and grain size of volcanic deposits can be determined from imagery; however,
22
23
24 color is not specific enough to identify the chemistry of volcanic rocks. XRF
25
26
27 measurements provide the bulk geochemical analysis of the material which, if fresh,
28
29
30
31 allows for the standard classification of the rock, providing valuable information of the
32
33
34 eruption style that produced the rock. VNIR spectra can confirm the XRF geochemical
35
36
37 classification by identifying minerals present which correspond to the rock type, for
38
39
40
41 example some spectral summary parameters (such as SH600_2, BD920_2, BD1300.,
42
43
44
45 LCPINDEX, HCPINDEX) show a correlation for mafic minerals in the more mafic chemical
46
47
48
49 compositions (Fig. 9).
50
51

52 The Askja eruption occurred less than 200 years ago and in an area that is quite cold
53
54
55
56 and dry; thus, we expected to see little evidence of alteration. The primary style of
57
58
59
60

alteration captured by VNIR was in the form of slight devitrification, captured by the 1400 nm and 1900 nm absorptions (e.g. summary parameter BD1900_2). This process is best



exemplified in the

Figure 9. Spearman correlation plot comparing which CRISM spectral parameters (top) correlate with bulk geochemistry and grain size of the samples. Red indicates negative correlation and blue indicates positive, white indicates no correlation.

samples with the higher silica content and smallest particles. Nearly all of the summary parameters which target clay minerals indicated the older material (lowest layers in the sampled stratigraphy) had the highest content of these minerals. This

1
2
3 higher concentration of clay minerals may have accumulated due to weathering in the
4
5
6
7 older layers over time.
8
9

10 The bulk geochemical compositions of the 1875 Askja layer C ash and a representative
11
12 ash layer are shown on Fig. 3 and match samples EET-4 and EET-6 most closely ¹⁰
13
14
15
16
17 though our analyses have slightly lower Na₂O wt. % than the published values.
18
19

20
21 There are few igneous minerals (3% plagioclase, 2% pyroxene, 0.5% iron oxide) in the
22
23 Askja ash and pumice as most of the deposit (94.5%) is glass ¹¹, which suggests the
24
25
26
27 dominant factor for influencing the VNIR spectra is likely not the minerals but the FeO wt.
28
29
30
31 % content of the glass ⁵³. The VNIR signature of glass is fairly featureless but shows
32
33
34 broad absorptions at 1100 nm and 1900 nm ⁵⁴. Additionally ⁵⁴ found an increase in FeO
35
36
37 wt. % in the glass affected the spectra in 3 specific ways: (1) a decrease in overall albedo,
38
39
40
41 (2) a flattening in the visible range with a near disappearance of the 800 nm shoulder, (3)
42
43
44 the slope between 1800 nm and 2400 nm will increase (Fig. 10). Samples EET-5 through
45
46
47
48 8 have similar albedo and iron content as the 100-125 μm and 200-180 μm grain size
49
50
51 experiments, whereas EET-1 through 4 were more consistent with the smaller grain size
52
53
54
55 experiments. This observation broadly matches the grain size data for our samples except
56
57
58
59
60

for EET-5 which has a high proportion of small grains and EET-3 which does not. The good correlation of this data suggest that the glassiness (as opposed to the mineral content) as well as the degree of mafic material is broadly responsible for the spectral characteristics seen in the VNIR range. The two major differences between our samples and the experiments were thus the likely inclusion of some crystals in the glassy matrix as well as wide variations in elemental oxides other than FeO (such as SiO₂) which may account for the higher albedo of EET-4 and EET-3 for the overall iron content.

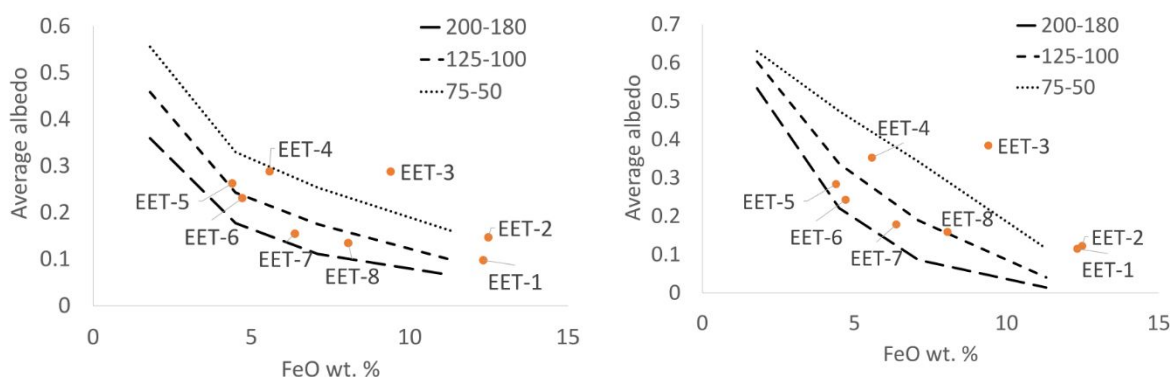


Figure 10. Graph illustrating the relationship between FeO content, grain size, and average spectral characteristics of glass. Grain size of experimental glass powders from Carli et al. (2015) are in mm and are represented by lines of different patterns. Our samples, which are mixtures of grain sizes, are the orange dots.

2. Microbial community- The microbiome of these sediments appears to be responding to two different sets of environmental drivers. The core microbiome varies significantly

1
2
3 with biological activity (ATP) and with free moisture (Fig. 7, Table 3) while the rare
4
5
6
7 microbiome varies significantly with the mineralogy and grain size of the sediment (Table
8
9
10 3).

11
12
13
14 The core microbiome's shift with increasing water content was probably responsible for
15
16
17 the increase in biological activity over the transect (Fig. 7). Members of the core
18
19
20 microbiome most responsible for this shift according to FDR-corrected one-way ANOVA
21
22
23 results include two ASVs from the phylum Bacteroidetes, family *Bacteroidia*: one from the
24
25
26 candidate genus OLB8 ($p=0.02$), which has also been found in a community of nitrate
27
28
29 reducers ⁵⁵ and one from the candidate family AKYH767 ($p=0.02$) (Fig. 7, Table S1).
30
31
32
33
34
35 Closest environmental hits for both ASVs are associated with nitrification, denitrification
36
37
38 and annamox (Table S1).
39
40

41
42 Changes in the total microbiome, when summed across phyla, also showed significant
43
44
45 changes in abundance of methanogens and methylotrophs/methanotrophs across the
46
47
48 transect (Fig. 8), with ASVs from both functional categories decreasing in abundance with
49
50
51 decreasing age of the parent material. This was surprising; whether or not methanogens
52
53
54
55
56 in this transect were producing methane, we would expect them to be more successful
57
58
59
60

1
2
3 and more prevalent in more anaerobic sediments with higher water content, which
4
5
6
7 describe the younger end of the transect. However, this may be due to an increase in
8
9
10 overall organic matter accumulation with age, providing increased access to acetic acid
11
12
13 or methanol at the older end of the transect. We also found an increase in abundance of
14
15
16 members of the Planctomycetes along the transect with increasing moisture content. This
17
18
19 was unsurprising, since the Planctomycetes have mainly been isolated from freshwater
20
21
22 or marine environments or moist soils and sediments ⁵⁶.
23
24
25
26

27
28 Shifts in the rare microbiome are more complicated to parse, but may be more relevant
29
30
31 to the field of astrobiology. Low-abundance (rare) ASVs or OTUs have in the past often
32
33
34 been excluded from analysis due to the prevailing belief that they are unlikely to be active,
35
36
37 but more recent studies have found that this component of the microbiome is functionally
38
39
40 important ^{46, 47}. The correlation of the rare microbiome in these samples with mineralogical
41
42
43 features of the sediment (i.e., chemical composition from XRF) (Table 3) suggests that
44
45
46 the low-abundance community is active and undergoes environmental selection, rather
47
48
49 than representing a non-active portion of the detectable microbiome such as a dormant
50
51
52 microbial seed bank or taphonomic signal (as discussed in ⁴⁵).
53
54
55
56
57
58
59
60

1
2
3
4 This shift in the rare microbiome with change in geochemistry could be due to differing
5
6
7 chemicals/nutrients provided by the sediment grains or the manner in which
8
9
10 microtopography of sand grains varies by composition. A number of studies have linked
11
12
13 individual microbial species or bulk abundance of microbes to particular mineral materials
14
15
16 that provide beneficial habitat (i.e. protection from radiation or temperature, availability of
17
18
19 moisture) such as the protected crevices of sand grains ^{44, 57} or micronutrients weathered
20
21
22 biotically or abiotically from rock or mineral ⁵⁸⁻⁶¹. However, there are relatively few studies
23
24
25 linking mineralogical properties of rocks and sediment to overall prokaryotic community
26
27
28 composition in plant-free environments, and most of these studies focus on the most
29
30
31 abundant community members. A study of prokaryotic colonization of pegmatitic granite
32
33
34 found that different community profiles were characteristic of different mineral crystals,
35
36
37 including community differences corresponding with varying levels of Al, Si and Ca oxide
38
39
40 derived from XRF readings ⁶². Endolithic microbial community structure in the Atacama
41
42
43 has been linked to rock porosity/physical structure rather than mineral chemistry and light
44
45
46 transmission properties, as water retention by rocks was the most important factor for
47
48
49 colonization ⁶³. In two studies of microbial colonization in sand grains of marine sediment
50
51
52
53
54
55
56
57
58
59
60

1
2
3 exposed to mechanical abrasion, prokaryotes grew preferentially in concave areas and
4
5
6
7 crevices and were mostly not found on smooth or convex surfaces ^{44, 57}. Probandt et al.
8
9
10 found that differences between the microbiome of individual sand grains were mainly due
11
12
13 to the presence of rare species, and each sand grain was not significantly different from
14
15
16
17 the bulk sediment once rare species were removed.
18
19
20

21 Over the compositional gradient at Askja, only the rare microbiome shifted in community
22
23
24 composition (i.e. relative abundance of individual ASVs) with changes in geochemistry.
25
26
27 This shift was correlated with the proportion of grains of the size 425-850 μm . This shift
28
29
30 may be due to the presence, or lack thereof, of crevices for microbes to occupy in this
31
32
33 particular grain size. Common eruption products of Plinian eruptions include rocks that
34
35
36
37 have increased porosity (pumice) as well as poorly rounded grains (ash fall).
38
39
40

41 *Relationship between grain size and shape and favorable habitat:* The two factors
42
43
44 unrelated to geochemistry that affected the microbial communities were the presence of
45
46
47 water and the proportion of rounded grains. Both of these factors are related to the
48
49
50 volcanic nature of the sediment. The samples which are older and contain more wind-
51
52
53 blown material (EET-1 through 3) are likely to contain more rounded grains due to the
54
55
56
57
58
59
60

1
2
3 bumping and grinding that grains experience when bouncing over the landscape.
4
5
6
7 Conversely, the young airfall deposits (EET-4 through 8) are more likely to retain their
8
9
10 crevices as the deposition process of volcanic ash and pumice is relatively gentle. Thus,
11
12
13 fresh volcanic products that have not been remobilized could be a particularly good
14
15
16
17 habitat.
18
19

20
21 Additionally, the fine-grained compacted ash layer (EET-4 and EET-5) may be serving
22
23
24 as an aquitard, allowing water to be trapped in the more porous layers above. Thus,
25
26
27 eruptions which progressed similar to the Askja 1875 eruption (highly explosive and
28
29
30 transitioning from ash into more pumice-rich, common in Plinian style eruptions) are
31
32
33 capable of rapidly creating non-rounded, water storing, protective habitat that may be
34
35
36
37 laterally very expansive, though not particularly thick.
38
39

40 41 42 *3. Implications for targeted sampling on Mars:* 43 44

45 Mars' early volcanic history may have been defined by more explosive volcanism as
46
47
48 evidenced by older regolith that is poorly consolidated and fine-grained ^{22, 25, 64, 65}. Most
49
50
51
52 of these eruptions are chemically basaltic in nature, similar to several eruptions preserved
53
54
55
56 on Earth such as Sunset Crater 1085 CE, Etna 122 BCE, Colima 1913, or the Fontana
57
58
59

1
2
3 unit 30 kya e.g. ^{17, 66, 67, 68}. There is also evidence for a widespread ash deposit in the Nili
4
5
6
7 Fossae and Jezero crater region, where the Mars 2020 rover will search for evidence of
8
9
10 biosignatures, stemming from the Syrtis Major volcanic province ²⁷. Additionally, there is
11
12
13
14 evidence from the Compact Reconnaissance Imaging Spectrometer for Mars (CRISM)
15
16
17 spectral imager that this reported ash layer is associated with clay mineralogy ⁶⁹.
18
19

20
21 The preservation of biological traces of chemoautotrophic and chemoorganotrophic
22
23 communities in volcanic sediments in Early Archaean fossils such as the Kitty's Gap Chert
24
25 suggests that if similar organisms existed in water-saturated volcanoclastic environments on Mars
26
27 their traces would also have been preserved, although their identification would likely require
28
29 sample return ⁷⁰. This is a promising avenue for biosignature investigation as it is possible that
30
31 Mars' window of habitability may not have been long enough for photosynthesis to develop ^{71, 72};
32
33 without the gross primary production rates provided by photosynthesis, it would be unlikely that
34
35 a rover could detect definitive biosignatures such as large organic deposits or macrofossils.
36
37
38

39
40 Given our observations and interpretation of samples from the Askja eruption, a mission
41
42 that has similar instrumentation to this study and the objective of searching for
43
44 biosignatures should prioritize samples that show evidence for fine-grained deposits
45
46
47 underlying a pumaceous air-fall. Our work shows that grains or clasts that have been
48
49
50 deposited in-place with limited re-mobilization, which would increase smoothness and
51
52
53
54
55
56
57
58
59
60

1
2
3 decrease crevices and protected niches, should be prioritized. Composition is perhaps
4
5
6
7 less of a driving factor than the physical nature of the deposits and the associated
8
9
10 geologic history.

11
12
13
14 While the focus of our research was on a specific volcanic analogue, the chemical and
15
16
17 physical properties we studied are universally variable within nearly all environments on
18
19
20 Mars. Thus our findings can be used to guide astrobiological sampling more broadly. For
21
22
23 example, the juxtaposition of water and fine-grained particles could occur from subsurface
24
25
26 disturbances of Martian sediment ⁷³⁻⁷⁶, or adsorbed water may signify regions which likely
27
28
29 contain near-surface aqueous activity ⁷⁷⁻⁷⁸. Furthermore, our findings could be paired with
30
31
32 measured data from Mars ⁷⁹ and recommendations of environments with high-likelihood
33
34
35 of preservation ⁸⁰ to maximize abundance of past-life. Our results also suggest that small
36
37
38 gradations over geological layers have a significant effect on which microbial community
39
40
41 members are present. Sampling across such sedimentary gradients on Mars would
42
43
44 provide a much wider variety of possible biosignatures and therefore a much greater
45
46
47
48
49
50
51 likelihood of detecting life.”
52
53
54
55
56
57
58
59
60

Conclusions:

By investigating analogous environments on Earth using the same instrumental capabilities available to planetary surface missions, we are able to devise sampling protocols that are likely to maximize biosignature payloads. Surfaces that appear homogenous at large scales may contain a huge variety of microenvironments and will need further investigation to select high-return sampling sites. This study illustrates how sites can be narrowed down using geological relationships as well as “stand-off” techniques that require little sample prep and have a fast turn-around time for results.

We chose a single small site that had several overlapping gradients (geochemical, grain size, hydrologic, and age) to illustrate the relative importance of these features as well as test how these features may be studied using analytical capabilities on Mars. We confirmed that overall biological activity correlates with free water in the sample and is linked to a core community including aerobic heterotrophs as well as putative denitrifiers, methanogens, and methylotrophs/methanotrophs. When excluding highly abundant ASVs (which include unlikely phyla for Mars) from our dataset, we see changes in the microbial community that respond to geological differences in the substrates. Specifically,

1
2
3 grain size, geochemistry, and deposit age/degree of transport affect the abundance and
4
5
6
7 composition of the microbiome, which may have implications for sampling missions.
8
9

10 Additionally, whereas the absolute age of the geologic units is fairly inconsequential,
11
12
13 the depositional history of the two units leads to greatly varied habitat. The older deposit
14
15
16 was comprised of wind-blown grains which and are more rounded compared to the
17
18
19 younger fall deposit above. Protected crevices in grains are common in Plinian eruption
20
21
22 deposits of all chemical compositions and thus should be sought out on sampling
23
24
25
26
27 missions. Based on these results, we recommend two sampling protocols:
28
29
30

31 1. A protocol to target highest levels of diversity and abundance should look for fresh
32
33
34 Plinian fall deposits with any sort of chemical gradient which can be identified using VNIR
35
36
37
38 at distance, confirmed with XRF and imagery at close range.
39
40

41 2. Further success could result from finding a sequence of deposits with very fine grain
42
43
44 size directly underneath more pumaceous fall deposits thus creating a small local aquifer
45
46
47
48 directly below a porous habitat. This suggests the deposit thickness might be an important
49
50
51
52 factor when scanning for ideal habitat.
53
54
55
56
57
58
59
60

ASSOCIATED CONTENT

Data Availability

This Targeted Locus Study project has been deposited at DDBJ/EMBL/GenBank under the accession KEEJ00000000. The version described in this paper is the first version, KEEJ01000000.

Supporting Information

The following files are available free of charge.

Supplemental Table 1. The raw visible near-infrared data for EET 1 through 8 (.xlsx)

Supplemental Table 2. Top 12 most abundant ASVs and their percent of total reads, with their SILVA database genus assignment and NCBI nucleotide database top environmental and culture hits for the sequence of that ASV (.xlsx)

ACKNOWLEDGMENT

We would like to acknowledge the funding sources that allowed us to gather and analyze this data; NASA award #NNX16AK13G, the NASA Postdoctoral Program, Georgia Institute of Technology, and the state of Georgia. Permitting was provided by the

1
2
3 Icelandic Centre for Research, Icelandic Institute of Natural History, and Vatnajökull
4
5
6
7 National Park. Some work was done at Georgia Institute of Technology (Georgia Tech)
8
9
10 with financial support from State of Georgia, USA. This work was performed in part at the
11
12
13 Georgia Tech Institute for Electronics and Nanotechnology, a member of the National
14
15
16
17 Nanotechnology Coordinated Infrastructure (NNCI), which is supported by the National
18
19
20
21 Science Foundation (Grant ECCS-1542174). Some of the research was carried out at the
22
23
24 Jet Propulsion Laboratory, California Institute of Technology, under a contract with the
25
26
27
28 National Aeronautics and Space Administration (80NM0018D0004).
29
30

31 32 ABBREVIATIONS 33

34
35 VNIR, visible near-infrared; XRF, x-ray fluorescent; EET, Elena's experimental transect;
36
37 ATP, adenosine triphosphate; PIXL, Planetary Instrument for X-ray Lithochemistry;
38
39 SHERLOC, Scanning Habitable Environments with Raman & Luminescence for Organics
40
41 & Chemicals; NASA, National Aeronautics and Space Administration; DNA,
42
43 deoxyribonucleic acid; ASD, Analytical Spectral Devicestm; EDTA,
44
45 Ethylenediaminetetraacetic acid; qPCR, quantitative polymerase chain reaction; ASV,
46
47 amplicon sequence variants; ANOVA, analysis of variance; PERMANOVA, permutational
48
49 multivariate analysis of variance
50

51 52 REFERENCES 53 54 55 56 57 58 59 60

1. Arnalds, O.; Dagsson-Waldhauserova, P.; Olafsson, H., The Icelandic volcanic aeolian environment: Processes and impacts—A review. *Aeolian Research* **2016**, *20*, 176-195.
2. Arnalds, O., Dust sources and deposition of aeolian materials in Iceland. **2010**.
3. Arnalds, O.; Gisladottir, F. O.; Orradottir, B., Determination of aeolian transport rates of volcanic soils in Iceland. *Geomorphology* **2012**, *167*, 4-12.
4. Thordarson, T.; Höskuldsson, Á., Postglacial volcanism in Iceland. *Jökull* **2008**, *58* (198), e228.
5. Edgett, K. S.; Lancaster, N., Volcaniclastic aeolian dunes: Terrestrial examples and application to Martian sands. *Journal of Arid Environments* **1993**, *25* (3), 271-297.
6. Sparks, R. S. J.; Wilson, L.; Sigurdsson, H., The pyroclastic deposits of the 1875 eruption of Askja, Iceland. *Philosophical Transactions of the Royal Society of London. Series A, Mathematical and Physical Sciences* **1981**, *299* (1447), 241-273.
7. Hartley, M. E.; Thordarson, T.; de Joux, A., Postglacial eruptive history of the Askja region, North Iceland. *Bulletin of Volcanology* **2016**, *78* (4), 28.
8. Carey, R.; Houghton, B.; Thordarson, T., Tephra dispersal and eruption dynamics of wet and dry phases of the 1875 eruption of Askja Volcano, Iceland. *Bulletin of Volcanology* **2010**, *72* (3), 259-278.
9. Huntingdon-Williams, A. G. Total grain size distribution and morphology characteristics of the Askja 1875 C tephra (Doctoral dissertation). **2018**.
10. Macdonald, R.; Sparks, R.; Sigurdsson, H.; Matthey, D.; McGarvie, D.; Smith, R., The 1875 eruption of Askja volcano, Iceland: combined fractional crystallization and selective contamination in the generation of rhyolitic magma. *Mineralogical Magazine* **1987**, *51* (360), 183-202.
11. Sigurdsson, H.; Sparks, R., Petrology of rhyolitic and mixed magma ejecta from the 1875 eruption of Askja, Iceland. *Journal of Petrology* **1981**, *22* (1), 41-84.
12. Mountney, N. P.; Russell, A. J., Sedimentology of cold-climate aeolian sandsheet deposits in the Askja region of northeast Iceland. *Sedimentary Geology* **2004**, *166* (3-4), 223-244.
13. Walker, G. P., Explosive volcanic eruptions—a new classification scheme. *Geologische Rundschau* **1973**, *62* (2), 431-446.

- 1
2
3
4 14. Walker, G., Plinian eruptions and their products. *Bulletin volcanologique* **1981**, *44*
5 (3), 223.
- 6
7 15. Walker, G. P.; Self, S.; Wilson, L., Tarawera 1886, New Zealand—a basaltic
8 plinian fissure eruption. *Journal of volcanology and geothermal research* **1984**, *21* (1-2),
9 61-78.
- 10
11 16. Williams, S. N., Plinian airfall deposits of basaltic composition. *Geology* **1983**, *11*
12 (4), 211-214.
- 13
14 17. Coltelli, M.; Del Carlo, P.; Vezzoli, L., Discovery of a Plinian basaltic eruption of
15 Roman age at Etna volcano, Italy. *Geology* **1998**, *26* (12), 1095-1098.
- 16
17 18. Sigurdsson, H.; Houghton, B.; McNutt, S.; Rymer, H.; Stix, J., *The encyclopedia*
18 *of volcanoes*. Elsevier: 2015.
- 19
20 19. Gualda, G. A.; Ghiorso, M. S., The Bishop Tuff giant magma body: an alternative
21 to the Standard Model. *Contributions to Mineralogy and Petrology* **2013**, *166* (3), 755-
22 775.
- 23
24 20. Jensen, B. J.; Pyne-O'Donnell, S.; Plunkett, G.; Froese, D. G.; Hughes, P. D.;
25 Sigl, M.; McConnell, J. R.; Amesbury, M. J.; Blackwell, P. G.; van den Bogaard, C.,
26 Transatlantic distribution of the Alaskan white river ash. *Geology* **2014**, *42* (10), 875-878.
- 27
28 21. Myers, M. L.; Wallace, P. J.; Wilson, C. J.; Watkins, J. M.; Liu, Y., Ascent rates
29 of rhyolitic magma at the onset of three caldera-forming eruptions. *American Mineralogist*
30 **2018**, *103* (6), 952-965.
- 31
32 22. Hynek, B. M.; Phillips, R. J.; Arvidson, R. E., Explosive volcanism in the Tharsis
33 region: Global evidence in the Martian geologic record. *Journal of Geophysical Research:*
34 *Planets* **2003**, *108* (E9).
- 35
36 23. Kerber, L.; Head, J. W.; Madeleine, J.-B.; Forget, F.; Wilson, L., The dispersal of
37 pyroclasts from ancient explosive volcanoes on Mars: Implications for the friable layered
38 deposits. *Icarus* **2012**, *219* (1), 358-381.
- 39
40 24. Michalski, J. R.; Bleacher, J. E., Supervolcanoes within an ancient volcanic
41 province in Arabia Terra, Mars. *Nature* **2013**, *502* (7469), 47-52.
- 42
43 25. Bandfield, J. L.; Edwards, C. S.; Montgomery, D. R.; Brand, B. D., The dual nature
44 of the martian crust: Young lavas and old clastic materials. *Icarus* **2013**, *222* (1), 188-199.
- 45
46
47
48
49
50
51
52
53
54
55
56
57
58
59
60

- 1
2
3
4 26. Morris, R. V.; Vaniman, D. T.; Blake, D. F.; Gellert, R.; Chipera, S. J.; Rampe,
5 E. B.; Ming, D. W.; Morrison, S. M.; Downs, R. T.; Treiman, A. H., Silicic volcanism on
6 Mars evidenced by tridymite in high-SiO₂ sedimentary rock at Gale crater. *Proceedings*
7 *of the National Academy of Sciences* **2016**, *113* (26), 7071-7076.
8
9
10 27. Kremer, C. H.; Mustard, J. F.; Bramble, M. S., A widespread olivine-rich ash
11 deposit on Mars. *Geology* **2019**, *47* (7), 677-681.
12
13
14 28. Fagents, S. A.; Wilson, L., Numerical modeling of ejecta dispersal from transient
15 volcanic explosions on Mars. *Icarus* **1996**, *123* (2), 284-295.
16
17 29. Kerber, L.; Forget, F.; Madeleine, J.-B.; Wordsworth, R.; Head, J. W.; Wilson,
18 L., The effect of atmospheric pressure on the dispersal of pyroclasts from martian
19 volcanoes. *Icarus* **2013**, *223* (1), 149-156.
20
21
22 30. Amador, E. S.; Cable, M. L.; Chaudry, N.; Cullen, T.; Gentry, D.; Jacobsen, M.
23 B.; Murukesan, G.; Schwieterman, E. W.; Stevens, A. H.; Stockton, A., Synchronous in-
24 field application of life-detection techniques in planetary analog missions. *Planetary and*
25 *Space Science* **2015**, *106*, 1-10.
26
27
28 31. Gentry, D. M.; Amador, E. S.; Cable, M. L.; Chaudry, N.; Cullen, T.; Jacobsen,
29 M. B.; Murukesan, G.; Schwieterman, E. W.; Stevens, A. H.; Stockton, A., Correlations
30 Between Life-Detection Techniques and Implications for Sampling Site Selection in
31 Planetary Analog Missions. *Astrobiology* **2017**, *17* (10), 1009-1021.
32
33
34 32. Hud, N. V., Our odyssey to find a plausible prebiotic path to RNA: the first twenty
35 years. *Synlett* **2017**, *28* (01), 36-55.
36
37
38 33. McKay, C. P.; Andersen, D.; Davila, A., Antarctic environments as models of
39 planetary habitats: University Valley as a model for modern Mars and Lake Untersee as
40 a model for Enceladus and ancient Mars. *The Polar Journal* **2017**, *7* (2), 303-318.
41
42
43 34. Bertagnolli, A. D.; Padilla, C. C.; Glass, J. B.; Thamdrup, B.; Stewart, F. J.,
44 Metabolic potential and in situ activity of marine Marinimicrobia bacteria in an anoxic
45 water column. *Environmental microbiology* **2017**, *19* (11), 4392-4416.
46
47
48 35. Grotzinger, J. P.; Sumner, D. Y.; Kah, L.; Stack, K.; Gupta, S.; Edgar, L.; Rubin,
49 D.; Lewis, K.; Schieber, J.; Mangold, N., A habitable fluvio-lacustrine environment at
50 Yellowknife Bay, Gale Crater, Mars. *Science* **2014**, *343* (6169), 1242777.
51
52
53
54
55
56
57
58
59
60

- 1
2
3
4 36. Ehlmann, B. L.; Mustard, J. F.; Fassett, C. I.; Schon, S. C.; Head III, J. W.; Des
5 Marais, D. J.; Grant, J. A.; Murchie, S. L., Clay minerals in delta deposits and organic
6 preservation potential on Mars. *Nature Geoscience* **2008**, *1* (6), 355-358.
- 7
8
9 37. Goudge, T. A.; Mustard, J. F.; Head, J. W.; Fassett, C. I.; Wiseman, S. M.,
10 Assessing the mineralogy of the watershed and fan deposits of the Jezero crater
11 paleolake system, Mars. *Journal of Geophysical Research: Planets* **2015**, *120* (4), 775-
12 808.
- 13
14
15 38. Allwood, A.; Clark, B.; Flannery, D.; Hurowitz, J.; Wade, L.; Elam, T.; Foote,
16 M.; Knowles, E. In *Texture-specific elemental analysis of rocks and soils with PIXL: The*
17 *Planetary Instrument for X-ray Lithochemistry on Mars 2020*, 2015 IEEE Aerospace
18 Conference, IEEE: 2015; pp 1-13.
- 19
20
21 39. Beegle, L.; Bhartia, R.; White, M.; DeFlores, L.; Abbey, W.; Wu, Y.-H.; Cameron,
22 B.; Moore, J.; Fries, M.; Burton, A. In *SHERLOC: scanning habitable environments with*
23 *Raman & luminescence for organics & chemicals*, 2015 IEEE Aerospace Conference,
24 IEEE: 2015; pp 1-11.
- 25
26
27 40. Wiens, R. C.; Maurice, S.; Rull Perez, F., The SuperCam remote sensing
28 instrument suite for the Mars 2020 rover mission: A preview. *Spectroscopy* **2017**, *32* (LA-
29 UR-17-26876).
- 30
31
32 41. Bennett, P. C.; Rogers, J. R.; Choi, W. J.; Hiebert, F. K., Silicates, Silicate
33 Weathering, and Microbial Ecology. *Geomicrobiology Journal* **2001**, *18* (1), 3-19.
- 34
35
36 42. Galand, P. E.; Casamayor, E. O.; Kirchman, D. L.; Lovejoy, C., Ecology of the
37 rare microbial biosphere of the Arctic Ocean. *Proc Natl Acad Sci U S A* **2009**, *106* (52),
38 22427-32.
- 39
40
41 43. Pedros-Alio, C., The rare bacterial biosphere. *Ann Rev Mar Sci* **2012**, *4*, 449-66.
- 42
43
44 44. Probandt, D.; Eickhorst, T.; Ellrott, A.; Amann, R.; Knittel, K., Microbial life on a
45 sand grain: from bulk sediment to single grains. *ISME J* **2018**, *12* (2), 623-633.
- 46
47
48 45. Lynch, M. D.; Neufeld, J. D., Ecology and exploration of the rare biosphere. *Nature*
49 *Reviews Microbiology* **2015**, *13* (4), 217-29.
- 50
51
52 46. Jousset, A.; Bienhold, C.; Chatzinotas, A.; Gallien, L.; Gobet, A.; Kurm, V.;
53 Kusel, K.; Rillig, M. C.; Rivett, D. W.; Salles, J. F.; van der Heijden, M. G.; Youssef, N.
- 54
55
56
57
58
59
60

1
2
3
4 H.; Zhang, X.; Wei, Z.; Hol, W. H., Where less may be more: how the rare biosphere
5 pulls ecosystems strings. *ISME J* **2017**, *11* (4), 853-862.

6
7 47. Shade, A.; Jones, S. E.; Caporaso, J. G.; Handelsman, J.; Knight, R.; Fierer,
8 N.; Gilbert, J. A., Conditionally rare taxa disproportionately contribute to temporal changes
9 in microbial diversity. *MBio* **2014**, *5* (4), e01371-14.

10
11 48. Ramirez, R. M.; Craddock, R. A., The geological and climatological case for a
12 warmer and wetter early Mars. *Nature Geoscience* **2018**, *11* (4), 230-237.

13
14 49. Hale, L.; Crowley, D., DNA extraction methodology for biochar-amended sand and
15 clay. *Biology and Fertility of Soils* **2015**, *51* (6), 733-738.

16
17 50. Love, M. I.; Huber, W.; Anders, S., Moderated estimation of fold change and
18 dispersion for RNA-seq data with DESeq2. *Genome Biol* **2014**, *15* (12), 550.

19
20 51. Viviano-Beck, C. E.; Seelos, F. P.; Murchie, S. L.; Kahn, E. G.; Seelos, K. D.;
21 Taylor, H. W.; Taylor, K.; Ehlmann, B. L.; Wiseman, S. M.; Mustard, J. F., Revised
22 CRISM spectral parameters and summary products based on the currently detected
23 mineral diversity on Mars. *Journal of Geophysical Research: Planets* **2014**, *119* (6), 1403-
24 1431.

25
26 52. Pyle, D. M., The thickness, volume and grainsize of tephra fall deposits. *Bulletin of*
27 *Volcanology* **1989**, *51* (1), 1-15.

28
29 53. Carli, C.; Serventi, G.; Sgavetti, M., VNIR spectral characteristics of terrestrial
30 igneous effusive rocks: mineralogical composition and the influence of texture. *Geological*
31 *Society, London, Special Publications* **2015**, *401* (1), 139-158.

32
33 54. Carli, C.; Roush, T.; Pedrazzi, G.; Capaccioni, F., Visible and Near-Infrared
34 (VNIR) reflectance spectroscopy of glassy igneous material: Spectral variation, retrieving
35 optical constants and particle sizes by Hapke model. *Icarus* **2016**, *266*, 267-278.

36
37 55. Chini, A.; Hollas, C. E.; Bolsan, A. C.; Venturin, B.; Bonassa, G.; Cantão, M. E.;
38 Ibelli, A. M. G.; Antes, F. G.; Kunz, A., Process Performance and Anammox Community
39 Diversity in a Deammonification Reactor Under Progressive Nitrogen Loading Rates for
40 Swine Wastewater Treatment. *Bioresource Technology* **2020**, 123521.

41
42 56. Fuerst, J. A.; Sagulenko, E., Beyond the bacterium: planctomycetes challenge our
43 concepts of microbial structure and function. *Nat Rev Microbiol* **2011**, *9* (6), 403-13.

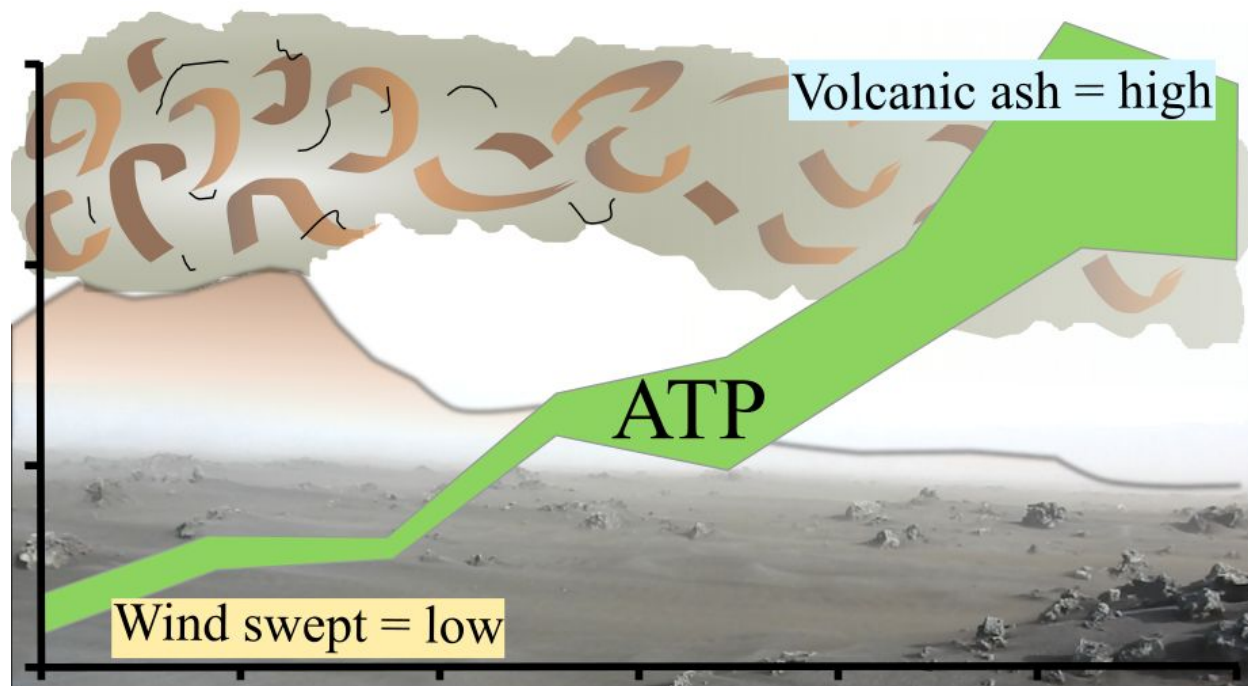
- 1
2
3
4 57. Weise, W.; Rheinheimer, G., Scanning electron microscopy and epifluorescence
5 investigation of bacterial colonization of marine sand sediments. *Microb Ecol* **1977**, *4* (3),
6 175-88.
7
8
9 58. Edwards, K. J.; Rutenberg, A. D., Microbial response to surface microtopography:
10 the role of metabolism in localized mineral dissolution. *Chemical Geology* **2001**, *180* (1-
11 4), 19-32.
12
13
14 59. Roberts, J. A., Inhibition and enhancement of microbial surface colonization: the
15 role of silicate composition. *Chemical Geology* **2004**, *212* (3-4), 313-327.
16
17
18 60. Rogers, J. R.; Bennett, P. C., Mineral stimulation of subsurface microorganisms:
19 release of limiting nutrients from silicates. *Chemical Geology* **2004**, *203* (1-2), 91-108.
20
21
22 61. Phillips-Lander, C. M.; Harrold, Z.; Hausrath, E. M.; Lanzirrotti, A.; Newville, M.;
23 Adcock, C. T.; Raymond, J. A.; Huang, S.; Tschauner, O.; Sanchez, A., Snow Algae
24 Preferentially Grow on Fe-containing Minerals and Contribute to the Formation of Fe
25 Phases. *Geomicrobiology Journal* **2020**, 1-10.
26
27
28 62. Gleeson, D. B.; Kennedy, N. M.; Clipson, N.; Melville, K.; Gadd, G. M.;
29 McDermott, F. P., Characterization of bacterial community structure on a weathered
30 pegmatitic granite. *Microb Ecol* **2006**, *51* (4), 526-34.
31
32
33 63. Meslier, V.; Casero, M. C.; Dailey, M.; Wierzchos, J.; Ascaso, C.; Artieda, O.;
34 McCullough, P. R.; DiRuggiero, J., Fundamental drivers for endolithic microbial
35 community assemblies in the hyperarid Atacama Desert. *Environ Microbiol* **2018**, *20* (5),
36 1765-1781.
37
38
39 64. Brož, P.; Hauber, E., A unique volcanic field in Tharsis, Mars: Pyroclastic cones as
40 evidence for explosive eruptions. *Icarus* **2012**, *218* (1), 88-99.
41
42
43 65. Rogers, A. D.; Warner, N. H.; Golombek, M. P.; Head III, J. W.; Cowart, J. C.,
44 Areally extensive surface bedrock exposures on Mars: Many are clastic rocks, not lavas.
45 *Geophysical research letters* **2018**, *45* (4), 1767-1777.
46
47
48 66. La Spina, G.; Clarke, A. B.; Vitturi, M. d. M.; Burton, M.; Allison, C.; Roggensack,
49 K.; Alfano, F., Conduit dynamics of highly explosive basaltic eruptions: The 1085 CE
50 Sunset Crater sub-Plinian events. *Journal of Volcanology and Geothermal Research*
51 **2019**, *387*, 106658.
52
53
54
55
56
57
58
59
60

- 1
2
3
4 67. Crummy, J. M.; Savov, I. P.; Navarro-Ochoa, C.; Morgan, D. J.; Wilson, M., High-
5 K Mafic Plinian Eruptions of Volcán de Colima, Mexico. *Journal of Petrology* **2014**, *55*
6 (11), 2155-2192.
7
8
9 68. Wehrmann, H.; Bonadonna, C.; Freundt, A.; Houghton, B. F.; Kutterolf, S.,
10 Fontana Tephra: a basaltic Plinian eruption in Nicaragua. *SPECIAL PAPERS-*
11 *GEOLOGICAL SOCIETY OF AMERICA* **2006**, *412*, 209.
12
13
14 69. Ehlmann, B. L.; Mustard, J. F., An in-situ record of major environmental transitions
15 on early Mars at Northeast Syrtis Major. *Geophysical research letters* **2012**, *39*(11).
16
17 70. Westall, F.; Foucher, F.; Cavalazzi, B.; de Vries, S. T.; Nijman, W.; Pearson,
18 V.; Watson, J.; Verchovsky, A.; Wright, I.; Rouzaud, J.-N.; Marchesini, D.; Anne, S.,
19 Volcaniclastic habitats for early life on Earth and Mars: A case study from ~3.5Ga-old
20 rocks from the Pilbara, Australia. *Planetary and Space Science* **2011**, *59*(10), 1093-1106.
21
22 71. Westall, F.; Foucher, F.; Bost, N.; Bertrand, M.; Loizeau, D.; Vago, J. L.;
23 Kminek, G.; Gaboyer, F.; Campbell, K. A.; Breheret, J. G.; Gautret, P.; Cockell, C. S.,
24 Biosignatures on Mars: What, Where, and How? Implications for the Search for Martian
25 Life. *Astrobiology* **2015**, *15*(11), 998-1029.
26
27 72. Cockell, C. S.; Balme, M.; Bridges, J. C.; Davila, A.; Schwenger, S. P.,
28 Uninhabited habitats on Mars. *Icarus* **2012**, *217*(1), 184-193.
29
30
31 73. De Toffoli, B.; Pozzobon, R.; Massironi, M.; Mazzarini, F.; Conway, S.; Cremonese, G., Surface
32 expressions of subsurface sediment Mobilization Rooted into a Gas Hydrate-Rich Cryosphere on
33 Mars. *Scientific reports* **2018**, *9*(1), 1-9.
34
35
36 74. Guidat, T.; Pochat, S.; Bourgeois, O.; Souček, O., Landform assemblage in Isidis Planitia, Mars:
37 Evidence for a 3 Ga old polythermal ice sheet. *Earth and Planetary Science Letters* **2015**, *411*, 253-267.
38
39
40 75. Hosein, R.; Haque, S.; Beckles, D. M., Mud volcanoes of Trinidad as astrobiological analogs for Martian
41 environments. *Life* **2014**, *4*(4), 566-585.
42
43
44 76. Skinner Jr, J. A.; Mazzini, A., Martian mud volcanism: Terrestrial analogs and implications for
45 formational scenarios. *Marine and Petroleum Geology* **2009**, *26*(9), 1866-1878.
46
47
48 77. McKay, C. P.; Stoker, C. R.; Glass, B. J.; Davé, A. I.; Davila, A. F.; Heldmann, J. L., ... Paulsen, G.,
49 The Icebreaker Life Mission to Mars: a search for biomolecular evidence for life. *Astrobiology* **2013**, *13*(4),
50 334-353.
51
52
53 78. Costard, F.; Forget, F.; Mangold, N.; Peulvast, J. P., Formation of recent Martian debris flows by melting
54 of near-surface ground ice at high obliquity. *Science* **2002**, *295*(5552), 110-113.
55
56
57
58
59
60

1
2
3
4
5
6
7
8
9
10
11
12
13
14
15
16
17
18
19
20
21
22
23
24
25
26
27
28
29
30
31
32
33
34
35
36
37
38
39
40
41
42
43
44
45
46
47
48
49
50
51
52
53
54
55
56
57
58
59
60

79. Edgar, L. A.; Gupta, S.; Rubin, D. M.; Lewis, K. W.; Kocurek, G. A.; Anderson, R. B.; ... Hardgrove, C., Shaler: in situ analysis of a fluvial sedimentary deposit on Mars. *Sedimentology* **2013**, *65*(1), 96-122.

80. McMahon, S.; Bosak, T.; Grotzinger, J. P.; Milliken, R. E.; Summons, R. E.; Daye, M.; ... Briggs, D. E. G., A field guide to finding fossils on Mars. *Journal of Geophysical Research: Planets* **2018**, *123*(5), 1012-1040.



1
2
3
4
5
6
7
8
9
10
11
12
13
14
15
16
17
18
19
20
21
22
23
24
25
26
27
28
29
30
31
32
33
34
35
36
37
38
39
40
41
42
43
44
45
46
47
48
49
50
51
52
53
54
55
56
57
58
59
60